Control Scheme for Phase Balancing and Reactive Power Support from Photovoltaic Inverters

Anastasis Charalambous, Lenos Hadjidemetriou, and Marios Polycarpou
KIOS Research and Innovation Center of Excellence and Department of Electrical and Computer Engineering
University of Cyprus
Nicosia, Cyprus
charalambous.anastasis@ucy.ac.cy

***Abstract*—The massive integration of intermitted renewable energy sources and the electrification of the transportation sector (e.g., electric vehicles) impose substantial challenges for the distribution system operators. These challenges include possible deterioration of the power quality, efficiency and stability of distribution grids. Therefore, the provision of ancillary services in a coordinated way is vital to alleviate these challenges, especially under high penetration of photovoltaics. This paper proposes a centralized control scheme for coordinating phase balancing and reactive power support services at the substation level of a distribution feeder. The distribution feeder controller is adaptively regulating the provision of phase balancing and reactive power support according to the loading conditions at the substation level. The proposed method is shown to provide significant benefits for the low voltage distribution grid in terms of power quality, stability, reduced energy losses and utilization of the network capacity.**

***Index Terms*—ancillary services, asymmetric loading, low voltage distribution grid, reactive power support, power quality**

I. Introduction

The reliability and stability of low voltage distribution grids (LVDGs) are starting to become a key concern due to the massive penetration of residential photovoltaics (PVs), the eventual increasing of load consumption (electrification of transportation and heating sector) and the highly asymmetrical loading conditions (i.e., single-phase connected loads). The motivation of the proposed centralized control scheme in this paper is to improve the power quality, efficiency and utilization of LVDGs by exploiting the capabilities of grid tied inverters.

Active management of LVDGs has been previously investigated in the literature. In [1], control actions are taken to regulate distributed generators to ensure that the LVDG operate within safe limits (i.e. voltage and thermal constraints). Optimization based control schemes (e.g., model predictive control) have also been proposed to minimize network losses and voltage variations by regulating active and reactive power of distributed resources [2], [3]. The studies in [1]–[3] consider that the LVDG is symmetrical; however this is not always the case in practice since a large number of consumers is single-phase connected.

Only few works in the literature consider phase balancing for LVDGs. There are several passive and active methods for compensating loading asymmetries [4]–[9]. Initially, active power filters have been proposed to compensate unbalanced currents [5]. However, the high capital cost of active power filters prohibit the wide adoption of these devices in LVDGs. Three-phase PV inverters already installed at the LVDG can be enhanced with additional capabilities to provide phase balancing at building level. The work in [7] proposes an advanced current controller that can regulate positive and negative sequence currents for compensating load asymmetries. However, asymmetric compensation can be implemented only at buildings that are equipped with PV systems. In [8], a centralized control scheme is developed to compensate for asymmetric conditions at the feeder level. In this work, the central controller coordinates several three-phase PV inverters and a battery energy system, which are enhanced with advanced capabilities for phase balancing compensation only. A control scheme for the coordination of both reactive power support and phase balancing in a microgrid was proposed in [9]. An advanced current reference generation controller is developed at PV inverters to share their available capacity between reactive power support and phase balancing according to the loading conditions. Then, a central controller coordinates the inverters in the microgrid using adaptive weights based on the inverters' availability. However, inappropriate tuning of the Proportional-Integral (PI) controllers at the central controller can lead to unstable conditions with significant consequences for the distribution system operator (DSO).

In this paper, a new centralized control scheme is proposed to compensate both reactive power and asymmetric loading conditions at a low voltage distribution feeder. A key contribution of this work is the stability analysis of the central controller developed in [9]. Motivated by this analysis, a new central controller is developed which can ensure stability. The modified central controller generates the reference signals for the three-phase PV inverters installed in a low voltage distribution feeder. The allocation of the ancillary services is based on adaptive weights that are dynamically updated according to the availability of each inverter. Furthermore, the

This work is undertaken as part of the project PVgnosis (P2P/SOLAR/0818/0007) funded under the umbrella of Horizon 2020 SOLAR-ERA.NET Cofund 2 (Cofund ERA-NET Action, N° 786483) and the Cyprus Research and Innovation Foundation. It is also supported by the European Regional Development Fund and the Republic of Cyprus through the Research and Innovation Foundation (Project: INTEGRATED/0916/0035). Further, this work is supported by the European Union's Horizon 2020 KIOS CoE project (No. 739551).

PV inverters are able to online prioritize the support of reactive power and phase balancing according to the loading conditions by adopting the advanced active and reactive power (PQ) controller developed in [9]. Therefore, the proposed central control scheme can provide significant benefits for the DSO in terms of power quality, efficiency and utilization of the network capacity without risking the stability of the grid.

The rest of the paper is organized as follows. Section II develops an advanced inverter controller for enabling ancillary services. The distribution feeder central controller is analyzed in Section III. Section IV illustrates the methodology using simulation results, while Section V provides some concluding remarks.

II. Advanced Photovoltaic Inverter

The proposed centralized control scheme requires that the PV inverter is able to exchange information with a central controller. More specifically, the inverter should receive the reference values for positive sequence reactive current injection (I^{+1*}_{Qinv}), negative sequence current injection ($\mathbf{i}^{-1*}_{inv}$) and the sharing constant that regulates the provision between the two services, as will be explained later. Further, the inverter should send its availability signals for phase balancing ($\hat{I}^{+1*}_{as-PB}$) and reactive power support ($\hat{I}^{+1*}_{as-Q}$), the positive sequence reactive current (I^{+1}_{Qinv}) and negative sequence current ($\mathbf{i}^{-1}_{inv}$) injected by each inverter to the central controller for properly allocating the services to each inverter. It should be noted that the inverter must provide the ancillary services without deviating its positive sequence active power production (P^{+1}_{inv}).

The structure of the advanced inverter controller is shown in Fig. 1(a). The advanced PV inverter is based on a decoupling network $\alpha\beta$ phase locked loop (DN$\alpha\beta$-PLL) for accurately extracting the phase angle [10], an enhanced current controller with the capability of injecting both positive and negative sequence currents [11] and an advanced PQ controller for enabling share provision of phase balancing and reactive power support services according to the loading conditions of the feeder [9]. The current controller is developed in two synchronous reference frames using PI controllers for accurately regulating positive and negative sequence currents. It should be noted that such current controller requires the decomposition of the inverter current into positive and negative sequences. For this reason, the decoupling network developed in [7] is used in the inverter's controller. The advanced PQ controller should receive the coordination signals from the central Low Voltage Distribution Feeder (LVDF) controller (see Section III) and should generate precisely the reference values of the positive and negative sequence currents. The PQ controller must also determine the allocation of the inverter's capacity for each ancillary service (reactive power support and phase balancing). To determine the capacity allocation, the inverter current ($\mathbf{i}_{inv}$) is analyzed in the synchronous reference frame (dq-frame). Therefore, the inverter should be able to inject both positive and negative sequence currents as follows,

$$\mathbf{i}_{inv} = \mathbf{i}^{+1}_{dq-inv} + \mathbf{i}^{-1}_{dq-inv} = \begin{bmatrix} i^{+1}_{d-inv} \\ i^{+1}_{q-inv} \end{bmatrix} + \begin{bmatrix} i^{-1}_{d-inv} \\ i^{-1}_{q-inv} \end{bmatrix}, \quad (1)$$

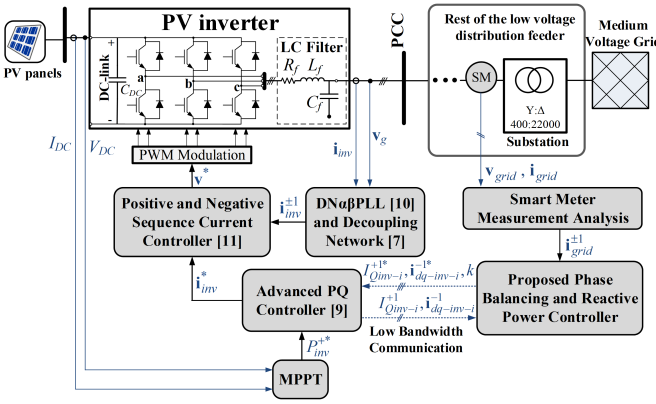

(a) Structure of the PV inverter and distribution feeder controller

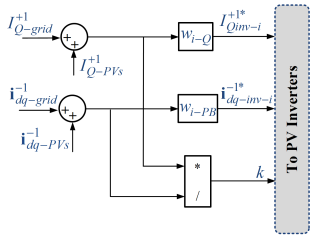

(b) Detailed structure of the proposed distribution feeder controller for phase balancing and reactive power support

Fig. 1. Schematic diagram of the PV inverter and feeder controller. (a) Overall structure of the PV inverter and distribution feeder controller. (b) Detailed structure of the proposed distribution feeder controller.

where $\mathbf{i}^{+1}_{dq-inv}$ represents the positive sequence current injection and $\mathbf{i}^{-1}_{dq-inv}$ represents the negative sequence injection expressed in the synchronous dq-frame. It should be highlighted that the d-axis positive sequence current (i^{+1}_{d-inv}) is associated with positive sequence active power (P^{+1}_{inv}) and should be not altered during the provision of ancillary services. The q-axis positive sequence current (i^{+1}_{q-inv}) is associated with reactive power support and the negative sequence current is related with the phase balancing service.

The PQ controller should ensure that the inverter current never violates its nominal current (I_{nom}) for securing the proper operation of the inverter. Further, it should determine the maximum allowable capacity for the positive sequence q-axis current and negative sequence current. Therefore, the maximum current that the converter can inject is given by

$$\begin{aligned} I_{nom} &= \sqrt{\left(i^{+1}_{d-inv}\right)^2 + \left(i^{+1}_{q-inv}\right)^2} + \sqrt{\left(i^{-1}_{d-inv}\right)^2 + \left(i^{-1}_{q-inv}\right)^2} \\ &= \sqrt{\left(i^{+1}_{d-inv}\right)^2 + \left(\hat{I}^{+1}_{Q-inv}\right)^2} + \hat{I}^{-1}_{PB-inv}, \end{aligned} \quad (2)$$

where $\hat{I}^{+1}_{Q-inv}$ represents the maximum current capacity allocated for reactive power support and $\hat{I}^{-1}_{PB-inv}$ represents the maximum current capacity allocated for phase balancing. The capacity for reactive power support can be expressed in term of the capacity for phase balancing as in (3) for enabling fair allocation between the two ancillary services.

$$\hat{I}^{+1}_{Q-inv} = k \cdot \hat{I}^{-1}_{PB-inv}. \quad (3)$$

The sharing constant (k) determines which of the ancillary services will be prioritized and it is estimated by the central LVDF controller. The sharing constant is calculated later on by considering the operating condition of the feeder, as will be explained in Section III. For instance, in case $k = 0$ the available capacity of the inverter can only be used for phase balancing service, while in case $k = 1$, the available capacity of the inverter is equally allocated to reactive power support and phase balancing services. Lastly, if $k > 1$ then priority is given to reactive power support. Once the available capacities for reactive power support and phase balancing are estimated, the PQ controller utilize them to limit the reference positive and negative sequence currents.

Finally, the PV inverter should report its availability for reactive power support and phase balancing to the central controller for coordination purposes. The availability of each PV inverter for reactive power support $(\hat{I}_{as-Q})$ and phase balancing $(\hat{I}_{as-PB})$ are estimated as follows:

$$\hat{I}_{as-Q} = \sqrt{(I_{nom})^2 - (i_{d-inv})^2} \tag{4}$$

$$\hat{I}_{as-PB} = |I_{nom}| - |i_{d-inv}|. \tag{5}$$

III. Low Voltage Distribution Feeder Controller

The LVDF controller coordinates the three-phase PV inverters for providing reactive power support and phase balancing according to the real-time loading conditions of the grid. A smart meter (SM) installed at the substation of the feeder sends its measurements for the positive sequence reactive power (Q^{+1}_{grid}) and the negative sequence current $(\mathbf{i}^{-1}_{grid})$ to the LVDF controller every 200 ms.

The allocation of the ancillary services is based on adaptive weights which are computed according to the available capacity of each inverter to provide either reactive power support or phase balancing as in,

$$w_{i-Q} = \frac{\hat{I}_{as-Q-i}}{\sum\limits_{n} \hat{I}_{as-Q-i}}, \quad w_{i-PB} = \frac{\hat{I}_{as-PB-i}}{\sum\limits_{m} \hat{I}_{as-PB-i}}, \tag{6}$$

where $\hat{I}_{as-Q-i}$ represents the available capacity for reactive power support of the i^{th} inverter, n represents the total number of inverters providing reactive power support, $\hat{I}_{as-PB-i}$ represents the i^{th} inverter capacity for phase balancing and m represents the number of inverters participating in phase balancing. In the literature, the generation of reference currents was previously implemented using PI controllers [9]. However, improper tuning can lead to unstable behavior for the LVDF controller. Therefore, investigating the stability of the overall system is a crucial aspect. Fig. 2 illustrates the closed-loop system considering only the phase balancing provision by the central controller that coordinates the negative sequence current of one three-phase PV inverter. It should be pointed out that the same analysis can be implemented for reactive power regulation, which leads to similar results.

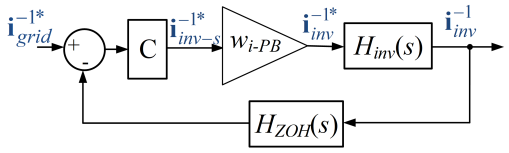

Fig. 2. Closed-loop schematic diagram of the distribution feeder controller.

The closed loop transfer function of a current controlled inverter is given by

$$H_{inv}(s) = \frac{G_{PI-CC}(s)G_D(s)G_f(s)}{1 + G_{PI-CC}(s)G_D(s)G_f(s)}. \tag{7}$$

The transfer function $G_D(s)$ below approximates all the delays that may occur in the control path of the inverter [12]:

$$G_D(s) = \frac{1}{T_d s + 1}. \tag{8}$$

where T_d $(1.5{\cdot}T_s)$ represents the total time delay of the control path (i.e., sampling, sensors, filters, PWM, etc.) and T_s represents the sampling period of the controller. The inverter is connected to the grid through an LC filter with transfer function

$$G_f(s) = \frac{1}{R_f + L_f s}, \tag{9}$$

where R_f (0.19 Ω) and L_f (15 mH) represent the filter resistor and inductor respectively. The transfer function of the PI controller used for current control of the inverter is given by,

$$G_{PI-CC}(s) = k_{p-cc} + k_{i-cc}\frac{1}{s}, \tag{10}$$

where k_{p-cc} and k_{i-cc} are the tuning parameters of the current controller. Therefore, the closed loop transfer function of the system with the central PI controller is given by,

$$H(s) = \frac{C(s)H_{inv}(s)}{1 + C(s)H_{ZOH}(s)H_{inv}(s)}, \tag{11}$$

where $H_{ZOH}(s)$ represents the sampling delays imposed by the reporting time of the smart meters installed at the substation. The $H_{ZOH}(s)$ is given by,

$$H_{ZOH}(s) = e^{-sT_{d-SM}}, \tag{12}$$

where T_{d-SM}(0.2 s) represents the sampling time of the corresponding smart meter. For analyzing the stability of the central controller, we express the delay in a rational form using Pade approximation. If the central LVDF controller is developed based on a PI controller, then the transfer function of the central controller $C(s)$ is given by,

$$C(s) = k_p + k_i\frac{1}{s}, \tag{13}$$

where k_p and k_i represents the proportional and integrator gains respectively. Fig. 3 shows the pole plot of the closed-loop transfer function $H(s)$ as the integrator gain k_i increases while the proportional gain was kept constant $(k_p = 0.2)$. As can be seen, the stability of the system deteriorates as the

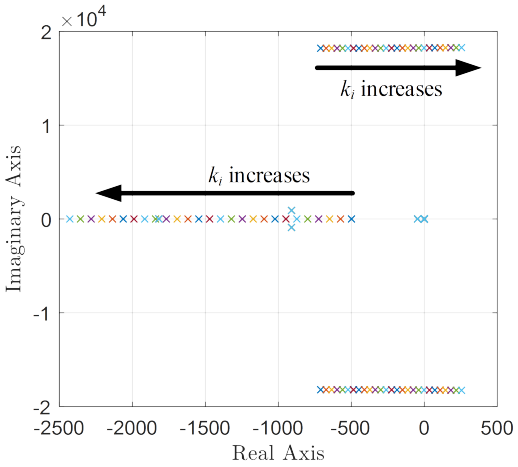

Fig. 3. Pole plot of $H(s)$ with k_i varies from 100-500.

integrator gain increases (i.e., the poles move to the right-half-plane). Therefore, the tuning of the central controller needs to be carefully selected.

To eliminate the risk of instability or large transients, the development of a LVDF controller that does not require any tuning parameters is pursued. Fig. 1(b) shows the schematic diagram of the proposed central controller and the exchange of information with the PV inverters. As can be seen, the reference signals $I^{+1*}_{Q-inv-s}$ and $\mathbf{i}^{-1*}_{inv-s}$ are generated by considering the grid measurements (I^{+1}_{Qgrid} and $\mathbf{i}^{-1}_{dq-grid}$) and the corresponding total provision of reactive power support and phase balancing from the PV inverters (I^{+1}_{Q-PVs}, $\mathbf{i}^{-1}_{dq-PVs}$) which are computed as:

$$I^{+1}_{Q-PVs} = \sum_{i=1}^{n} I^{+1}_{Q-inv-i}\ , \quad \mathbf{i}^{-1}_{dq-PVs} = \sum_{i=1}^{n} \mathbf{i}^{-1}_{dq-inv-i}, \quad (14)$$

where $I^{+1}_{Q-inv-i}$ represents the positive sequence reactive current injection from the i^{th} inverter, $\mathbf{i}^{-1}_{dq-inv-i}$ represents the negative sequence current injection from the i^{th} inverter and n represents the total number of inverters participating in the ancillary services provision. The online computation of the sharing constant for fair allocation between reactive power support and phase balancing is derived according to the operating conditions as in,

$$k = \frac{I^{+1}_{Q-PVs} + I^{+1}_{Q-grid}}{\mathbf{i}^{-1}_{grid} + \mathbf{i}^{-1}_{PVs}}, \quad (15)$$

where I^{+1}_{Q-PVs} and I^{+1}_{Q-grid} represent the total reactive current injected by the PV inverters and the reactive current measured at the substation respectively.

IV. Simulation Based Case Study

A four wire LVDF is modeled in MATLAB/Simulink to investigate the effectiveness of the proposed controller. The feeder serves several single-phase and three-phase consumers as shown in Fig. 4. A 10 kVA peak three-phase PV system is considered for each three-phase consumer in which the inverter controller is enhanced with the advanced functionalities as demonstrated in Section II. The LVDF controller receives the measurements from the smart meter installed at the substation and generates the coordination signals for reactive power support and phase balancing for each PV inverter. Finally, during the case studies, each PV plant generates 2 kW.

In this case study, the steady state performance of the proposed LVDF controller is investigated. Fig. 5(a) illustrates the grid current $\mathbf{i}_{grid}$ and positive sequence reactive power Q^{+1}_{grid} measured at the high voltage side of the substation when the LVDF controller is deactivated. The LVDF controller is activated at $t = 1.8$ s and according to the loading conditions $k = 2$. As can be seen in Fig. 5(b), when the LVDF controller is activated, the grid current becomes symmetrical and $Q^{+1}_{grid} = 0$ kVAr. The phase balancing operation can also be seen from the oscillations on reactive power that are eliminated when the LVDF controller is activated. Although in this case, the sharing constant prioritize reactive power provision, the capacity of the inverter is greater than the total capacity needed for ancillary services hence both reactive power support and phase balancing are provided. In case the capacity of the PV inverters is less than the required, then priority would be given to reactive power support and if there was additional capacity would be utilised for phase balancing.

The transient performance of the LVDF controller is shown in Fig. 6. In this case study, the sharing constant is set to a range of values ($k \in [0,\ 100]$) to show the different capabilities of the LVDF controller and the advanced capabilities of the PV inverters. Initially, the LVDF controller is deactivated as a result the grid current is asymmetrical due to the connection of single-phase loads. Further, the loads consume mean reactive power of 20 kVAr. At $t = 1.6$ s the LVDF controller is activated with $k = 0$. As can be seen, the grid currents are perfectly symmetrical due to the injection of asymmetrical currents from the PV inverters (i.e., provision of phase balancing). It should be noted that Fig. 6 illustrates only the inverter current ($\mathbf{i}_{inv}$) of one PV system only. The phase balancing compensation is also demonstrated by the elimination of the double frequency oscillations on active (P_{grid}) and reactive (Q_{grid}) power at the grid during $1.6 < t < 1.8$ s. At $t = 1.8$ s the sharing constant is set to 100. As shown in Fig. 6, reactive

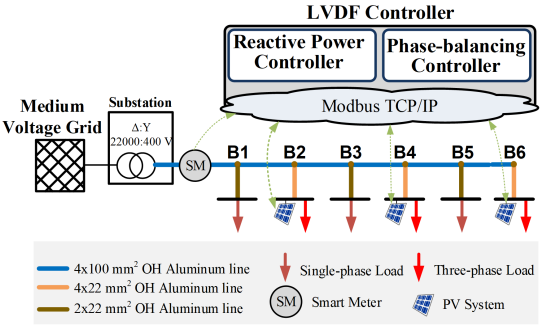

Fig. 4. Low voltage distribution feeder with LVDF controller.

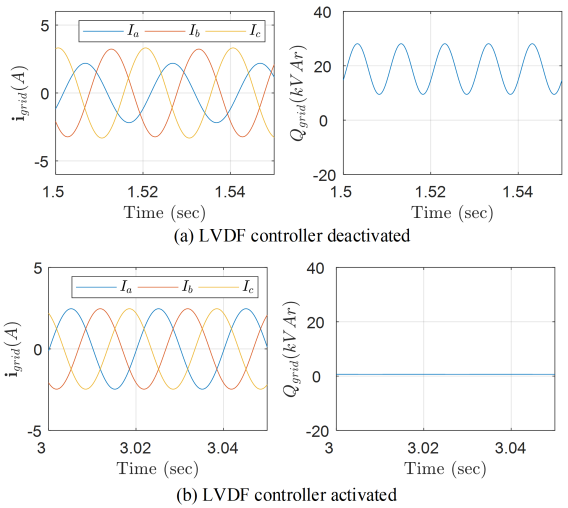

(a) LVDF controller deactivated

(b) LVDF controller activated

Fig. 5. Steady state operation of the LVDF controller.

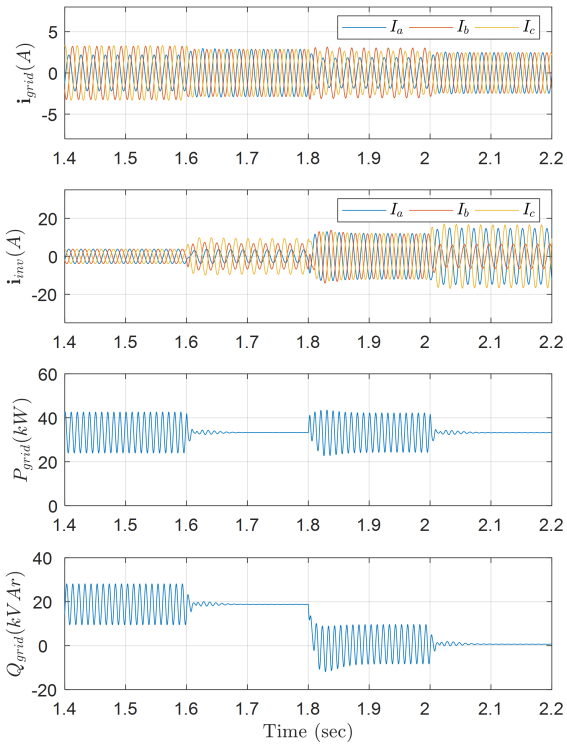

Fig. 6. Transient operation of the LVDF controller.

power support is provided from the PV inverters which in this case are injecting balanced currents. Although the grid current is asymmetrical, the mean reactive power at the grid becomes zero. However, intense oscillations are observed on active and reactive power that deteriorate the power quality of the grid. Finally, at $t = 2$ s the sharing constant is set to 1 (i.e., equal provision of reactive power support and phase balancing). As can be seen, the reactive power exchange with the grid remains zero and the double frequency oscillations on active and reactive power are eliminated. Therefore, in this case the PV inverters provide support on both services for improving power quality, efficiency and utilization of the network capacity. It is worth pointing out that when providing ancillary services, the active power production of the PV plants is not altered while their nominal peak current ($I_{nom} = 20$ A) is not exceeded.

V. Conclusions

A LVDF controller is proposed for the provision of reactive power support and phase balancing at the substation level. The performed investigation demonstrates that the proposed LVDF controller improves significantly the operation of the distribution grid in terms of power quality, energy losses and effective utilization of its capacity. Further, the proposed control scheme shows improved stability characteristics compared with previous methods due to the elimination of integral controllers. Finally, the operation of the proposed LVDF controller requires advanced functionalities to be enabled in the controller of the PV inverters for the provision and online allocation of the ancillary services.

References

[1] C. Feng, Z. Li, M. Shahidehpour, F. Wen, W. Liu, and X. Wang, "Decentralized short-term voltage control in active power distribution systems," *IEEE Trans. Smart Grid*, vol. 9, no. 5, pp. 4566–4576, Sep. 2018.

[2] B. A. Robbins and A. D. Domínguez-García, "Optimal reactive power dispatch for voltage regulation in unbalanced distribution systems," *IEEE Trans. Power Systems*, vol. 31, no. 4, pp. 2903–2913, July 2016.

[3] G. Valverde and T. Van Cutsem, "Model predictive control of voltages in active distribution networks," *IEEE Trans. Smart Grid*, vol. 4, no. 4, pp. 2152–2161, Dec. 2013.

[4] B. R. Pereira, G. R. M. da Costa, J. Contreras, and J. R. S. Mantovani, "Optimal distributed generation and reactive power allocation in electrical distribution systems," *IEEE Trans. Sustainable Energy*, vol. 7, no. 3, pp. 975–984, July 2016.

[5] M. M. Hashempour, M. Savaghebi, J. C. Vasquez, and J. M. Guerrero, "A control architecture to coordinate distributed generators and active power filters coexisting in a microgrid," *IEEE Trans. Smart Grid*, vol. 7, no. 5, pp. 2325–2336, Sep. 2016.

[6] L. Wang, C. Lam, and M. Wong, "Selective compensation of distortion, unbalanced and reactive power of a thyristor-controlled lc -coupling hybrid active power filter," *IEEE Trans. Power Electron.*, vol. 32, no. 12, pp. 9065–9077, Dec. 2017.

[7] L. Hadjidemetriou, L. Zacharia, and E. Kyriakides, "Flexible power control scheme for interconnected photovoltaics to benefit the power quality and the network losses of the distribution grid," in *Proc. IEEE ECCE Asia*, Kaohsiung 2017, pp. 93–98.

[8] L. Hadjidemetriou, A. Charalambous, and E. Kyriakides, "Control scheme for phase balancing of low-voltage distribution grids," in *Proc. SECT*, Porto 2019, pp. 1–6.

[9] A. Charalambous, L. Hadjidemetriou, L. Zacharia, A. D. Bintoudi, A. C. Tsolakis, D. Tzovaras, and E. Kyriakides, "Phase balancing and reactive power support services for microgrids," *Applied Sciences*, vol. 9, no. 23, p. 5067, Nov. Nov. 2019.

[10] L. Hadjidemetriou, E. Kyriakides, and F. Blaabjerg, "A robust synchronization to enhance the power quality of renewable energy systems," *IEEE Trans. Ind. Electron.*, vol. 62, no. 8, pp. 4858–4868, Aug. 2015.

[11] M. Reyes, P. Rodriguez, S. Vazquez, A. Luna, R. Teodorescu, and J. M. Carrasco, "Enhanced decoupled double synchronous reference frame current controller for unbalanced grid-voltage conditions," *IEEE Trans. Power Electron.*, vol. 27, no. 9, pp. 3934–3943, Sep. 2012.

[12] Z. Branislav, T. Angela, G. Xavier, P. Rastislav, and S. Ligui, "Experimental evaluation of pi tuning techniques for field oriented control of permanent magnet synchronous motors," *Advances in Electrical and Electronic Engineering*, vol. 5, no. 1, pp. 114–119, June 2011.